

Ramsey Interferences and Spin Echoes from Electron Spins Inside a Levitating Macroscopic Particle

T. Delord, P. Huillery, L. Schwab, L. Nicolas, L. Lecordier, and G. Hétet

Laboratoire Pierre Aigrain, Ecole normale supérieure, PSL Research University, CNRS, Université Pierre et Marie Curie, Sorbonne Universités, Université Paris Diderot, Sorbonne Paris-Cité, 24 rue Lhomond, 75231 Paris Cedex 05, France



(Received 23 January 2018; published 30 July 2018)

We report on observations of Ramsey interferences and spin echoes from electron spins inside a levitating macroscopic particle. The experiment is realized using nitrogen-vacancy (NV) centers hosted in a micron-sized diamond stored in a Paul trap both under atmospheric conditions and under vacuum. Spin echoes are used to show that the Paul trap preserves the coherence time of the embedded electron spins for more than microseconds. Conversely, the NV spin is employed to demonstrate high angular stability of the diamond even under vacuum. These results are significant steps towards strong coupling of NV spins to the rotational mode of levitating diamonds.

DOI: [10.1103/PhysRevLett.121.053602](https://doi.org/10.1103/PhysRevLett.121.053602)

Being able to prepare arbitrary motional quantum states of massive oscillators will be an important step forward for modern quantum science [1]. Tremendous efforts are made towards this goal with experimental platforms ranging from clamped nanofabricated devices [2–4] to levitating objects [5,6]. One recently proposed way to engineer motional states consists in coupling atomic spins to the motion of macroscopic objects using magnetic fields [7–14]. The idea is to exploit the pointlike character of single atomic electrons and their magnetic sensitivity to detect and also to couple them to the motion of the oscillator. The resulting spin-dependent force on the object could for instance be used to cool the oscillator motion down, to generate motional cat states, or to entangle the spin with the mechanical oscillator [12,15]. The platform can then be employed for sensing the mechanical zero-point fluctuations [10] and for more fundamental tests of quantum mechanics [16–18].

Amongst the vast range of mechanical oscillators, particles levitating in harmonic potentials are being investigated widely. They have shown record high quality factors, stemming mostly from the absence of clamping losses [5,6,19]. They also enable efficient tuning of the mechanical properties. Lowering the trap stiffness after cooling the center-of-mass mode could for instance increase the ground state wave-function spread to several microns, offering prospects for optical manipulations of the wave packet [20]. There have also been several experiments that have achieved spin readout of nitrogen-vacancy (NV) centers hosted in diamonds that were trapped both in liquid [21,22] and under vacuum [23–26], which are important steps towards coupling spins to macroscopic particles' motion. The main quantum physics tools for engineering internal electronic and motional states—namely, Ramsey interferometry and spin echoes—are, however, still elusive for trapped macroscopic particles, stemming mostly from

the high degree of control required on the particle external and internal degrees of freedom (d.o.f.).

Ramsey interferometry and spin echoes have been the workhorse for many experiments in atomic physics in recent decades. They have allowed control of the environment of electronic spins with atomic ensembles or single atoms for decades. Such measurements tools are also essential for prospective spin coupling to the motional state of macroscopic oscillators [10,15,27]. In this Letter, we demonstrate contrasting Rabi and Ramsey oscillations as well as spin echoes from spins inside a macroscopic levitating particle under atmospheric conditions and under vacuum. The experiment consists of manipulating the spin of NV centers within a microdiamond levitating in a ring Paul trap. Although high voltages are used around small heavily charged diamonds, no differences between the longitudinal and transverse coherence times T_1 and T_2^* of the NV spins inside and outside the trap are observed. Importantly, our experiments are performed in the presence of a large magnetic field, which demonstrates coherent control over angularly stable particles, an important prerequisite for recently proposed experiments on spin-mechanical coupling using the rotational modes [12,14].

Figure 1 shows the principle of the experiment. A micron-sized, gold-plated tungsten ring trap [28–30] is used both for trapping micron-sized diamonds and for generating the oscillating transverse magnetic field that drives NV center spins. A green laser is focused onto the diamond and the photoluminescence (PL) from the embedded NV centers is collected using the same objective and directed to an avalanche photodiode. A permanent magnet is brought in the vicinity of the trap to lift the degeneracy between the $|m_s = \pm 1\rangle$ NV electronic spin states. The NV centers are polarized using around 1 mW

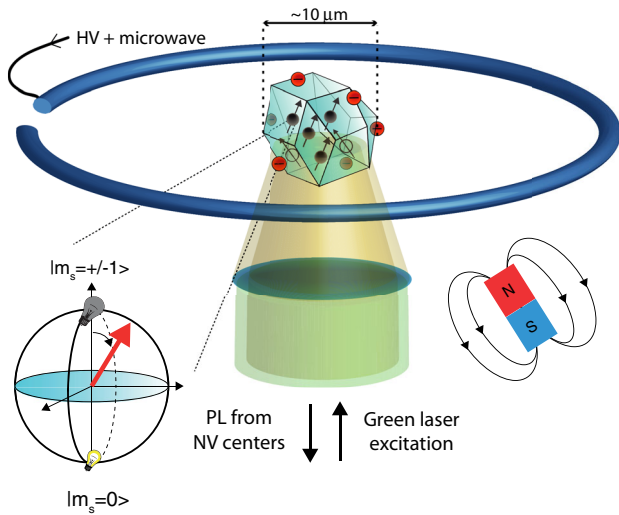


FIG. 1. Schematics of the experiment. A charged micron-sized diamond containing NV centers is levitating in a Paul trap. The spin properties of the NV centers are analyzed using confocal microscopy with both oscillating and static magnetic fields. The trap can be operated under vacuum or atmospheric conditions.

of green laser and a maximum of 20 dBm of microwave power can be brought to the ring to drive the electronic spins. More details on the experiment, such as the number of NV centers and the diamond shape and size, are presented in Refs. [25,31] and Sec. I of the Supplemental Material (SM) [32]. Compared to the experiment performed in Ref. [25], the ring trap is 4 times smaller. We measured it to be $180 \mu\text{m}$ in diameter, which means that both the confinement and microwave powers at the trap center are greatly increased. Using such a tiny ring trap is crucial for reaching angular stability under vacuum.

Before realizing experiments with levitating particles, an in-depth study of the spin properties of NVs from diamonds that are cast on a quartz plate was realized beforehand. It is presented in Sec. II of the SM [32]. Since at present we cannot compare the properties of the same particle in and out of the trap as was done in Ref. [41], such a characterization step was mandatory to estimate the influence of the trap on the NV photophysical properties.

To realize spin coherent control, we apply a magnetic field that lifts the degeneracy between the state $|m_s = \pm 1\rangle$. As discussed in Sec. II of the SM [32], crystal strain partially lifts the degeneracy between the $|m_s = \pm 1\rangle$ state and possibly also between the four orientations of the NV if anisotropic. Applying a magnetic field will thus ensure an addressing of a more homogeneous class of NV centers. This will in turn reduce the ESR linewidth and improve the measured coherence time. Applying a magnetic field, however, means that the measurement must be realized on angularly stable particles (see Secs. II and III of the SM [32]). Figure 2(a) shows an ESR taken under atmospheric pressure in the presence of a magnetic field of about 50 G. Eight distinctive dips are observable, corresponding to the

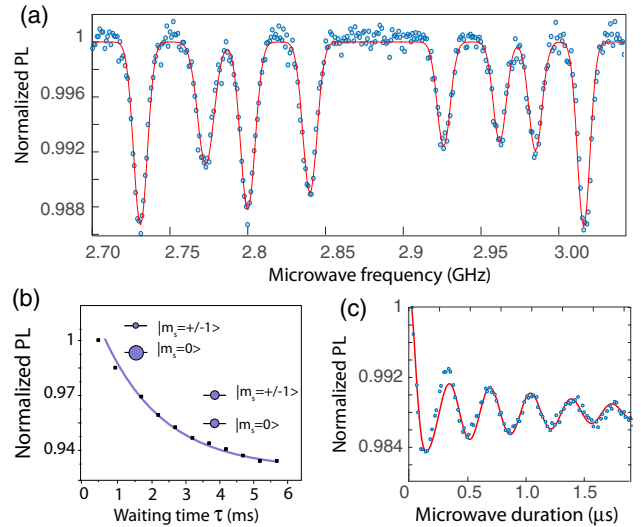


FIG. 2. (a) Electronic spin resonance spectrum, (b) longitudinal spin relaxation, and (c) Rabi oscillations from NV centers in a diamond monocrystal levitating in a Paul trap under ambient conditions.

projection of the magnetic field over the four NV quantization axes inside the levitating diamond crystal. When comparing this with typical ESR widths and contrasts obtained with deposited diamonds [32], we conclude that the diamond does not rotate over the course of the measurement. This angular stability was interpreted in Ref. [31] to be due to a trapping mechanism akin to that of the center of mass when the shape of the diamond particles is asymmetrical (a SEM image of the diamonds is shown in Sec. I of the SM [32]). Here, the laser and microwave signals are just below the saturation of the transition; we then expect the ESR width to be determined mainly by the coupling to the diamond strain and coupling to impurities [42,43]. Each ESR dip is indeed well approximated by a Gaussian function with an average width σ of about 8 MHz. We thus expect T_2^* times of about 50 ns.

Another important quantity is the lifetime of the spin population in the $|m_s = 0\rangle$ state, the so-called T_1 time, which can be as long as milliseconds in bulk diamonds at room temperature. For optomechanical experiments involving spins, ideally the population lifetime time should equal half of the transverse coherence time for an optimum spin coupling to the motion coupling [8,27]. It is thus important that the T_1 time is as large as possible, and possibly limited by electron to phonon processes, as can be the case in pure bulk diamonds [44,45]. Figure 2(b) shows a measurement of the T_1 time of NV centers in the levitating diamond. The typical parameters of a sequence are detailed in Sec. II of the SM [32]. The evolution of the PL as a function of the waiting time shows exponential decay of the photoluminescence, indicating that the NV centers remain in the $|m_s = 0\rangle$ state for more than 3 ms. Such a long T_1 highlights two features of this experiment: in our diamonds,

the T_1 is close to typical bulk values. Compared to nano-diamonds, it is thus not shortened by coupling of the NV spins to surface dangling bonds of paramagnetic impurities [46]. Second, the Paul trap does not significantly modify the longitudinal spin properties of the NV centers. This offers the prospect of increasing T_2^* towards millisecond-long coherence times via dynamical decoupling techniques [47].

We now demonstrate coherent control on many NV centers in the trapped diamond. We choose the extremal $|m_s = 0\rangle$ to $|m_s = +1\rangle$ ESR line and apply a sequence of microwave pulses with varying duration at this microwave frequency. Figure 2(c) shows a plot of the normalized PL rate as a function of the microwave duration. Rabi oscillations are observed for more than $1\ \mu\text{s}$. The Rabi envelope decay is characteristic of the environmental noise spectrum [48] (see Sec. II of the SM [32]). However, the observed damping time does not give direct access to the T_2^* time. When the Rabi frequency is lower than the ESR width, less spectrally distinct NV centers' spin and/or more classes of NV to nuclear spin couplings within the ESR profile are being excited, which effectively decreases the Rabi decay rate. The decay time can in fact be longer than the T_2^* time and is determined to a large extent by the employed microwave power [49–51] (see also Sec. II of the SM [32]).

We now proceed with the demonstration of Ramsey interference with the NV spins in order to estimate the T_2^* time of the NVs in the levitating diamond. Ramsey interference is generally realized on two-level systems driven by two $\pi/2$ pulses separated by a time τ , as depicted in Fig. 3(a). To probe the coherence time, we detune the microwave and scan the time interval τ using levitating diamonds. Figure 3(a) shows the change in the

photoluminescence rate as a function of the free precession time τ for three different detunings from the central line and $\pi/2$ microwave pulse duration of 50 ns. Traces (i), (ii), and (iii) correspond to detunings $\Delta/2\pi$ of 11, 15, and 20 MHz, respectively. A pronounced oscillation of the PL is observed as a function of the precession time, and the precession period closely follows the inverse of the microwave detunings. A Gaussian fit to the data yields decay times of 45 ± 4 , 50 ± 5 , and 45 ± 3 ns, respectively. Using a T_2^* value of 47 ns gives a corresponding ESR width of 9.4 MHz, very close to our measured ESR width value.

To probe even further the capability of the Paul trap to preserve the electronic spin coherence, we now apply the spin-echo sequence depicted in Fig. 3(b). In the high pressure, high temperature diamond samples we use, temporal inhomogeneity resulting from nuclear spin impurities typically shift the energy of the NV centers' spins and affect their coherence on microsecond timescales (see Sec. II of the SM [32]), so applying a π pulse between the two $\pi/2$ pulses can compensate for the associated spin dephasing. The result of the measurement is shown Fig. 3(b)(i), where the PL rate is plotted as a function of the precession time. The inset shows the corresponding resonant Ramsey curve. The PL rate change is well approximated by a decaying exponential curve, from which we extract a decay rate of $1.4\ \mu\text{s}$ [49,52]. Surprisingly, these values are similar to that observed with deposited diamonds (see Sec. II of the SM [32]). We conclude that the trap does not affect significantly the transverse spin coherence.

The above experiments were realized under ambient conditions. Typical optomechanical applications, however, require operation in the underdamped regime—that is, in the regime where the collision rate with surrounding gas particles is smaller than the macromotion frequency of the trapped diamond. As shown in Sec. I of the SM [32], the underdamped regime is reached in the millibar range in our experiment. To efficiently control the spins then, an important signature would be the presence of the four stable spin orientations in the ESR, which has not been observed so far in the underdamped regime. Indeed, angular stability is much more challenging to achieve under vacuum, where the trapping frequencies are lower and any nonconservative force heats up the particle motion significantly [32].

Figure 4(a) shows an ESR spectrum taken under 1.5 mbar of vacuum pressure. Although the ESR contrast is, on average, reduced due to the smaller employed microwave and laser powers (see Sec. II of the SM [32]), the presence of eight distinctive Gaussian dips shows again that this diamond did not rotate significantly over the course of the measurement. The key ingredient to observing angular stability under vacuum was the fabrication of a small highly confining ring trap to counteract nonconservative forces, such as the laser radiation pressure torque on asymmetric particles [31] or residual micromotion. This observation means that coherent driving on one NV orientation is

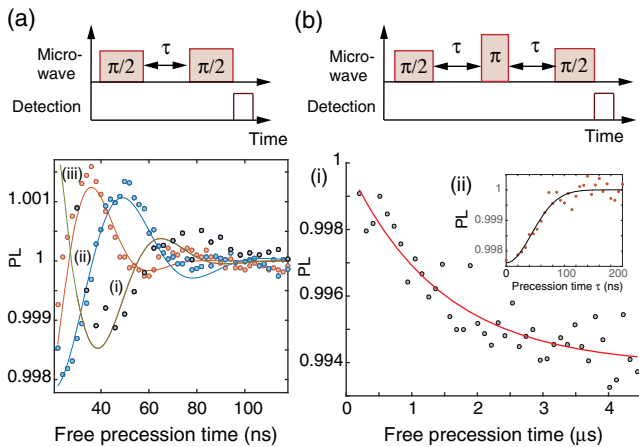


FIG. 3. (a) (Top panel) Sequence used for measuring Ramsey oscillations with NV centers. (Bottom panel) Ramsey oscillations from NV centers in a levitating diamond measured for three microwave detunings $\Delta/2\pi$ from the ESR line under atmospheric conditions. (b) Spin-echo sequence and normalized photoluminescence as a function of precession time for the echo sequence [trace (i)] and Ramsey measurements with a resonant microwave tone [trace (ii)].

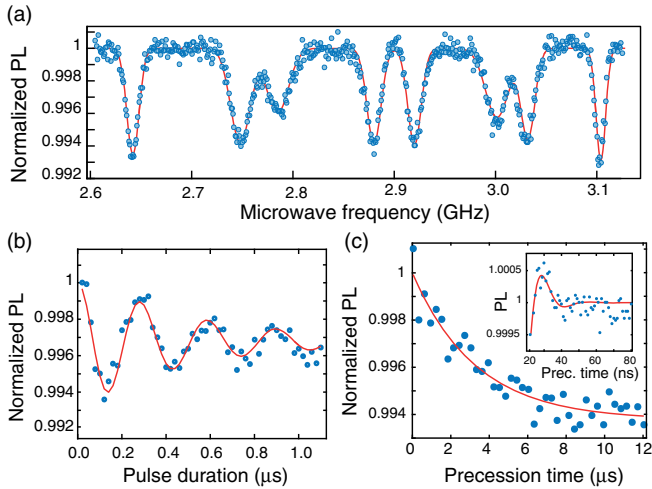


FIG. 4. Spin control of NV centers in diamonds levitating in the underdamped regime. (a) Electronic spin resonance, (b) Rabi oscillations and (c) spin echo, and (inset) Ramsey measurements. All measurements are conducted under about 1 mbar of vacuum pressure.

possible. Figure 4(b) indeed shows Rabi oscillations taken at 1 mbar of vacuum pressure, where contrasted coherent oscillations are observed with decay times similar to that measured under atmospheric conditions. Figure 4(c) shows spin-echo and Ramsey (inset) measurements. Ramsey measurements are taken at a detuning of 23 MHz. A clear variation of the PL is seen from 20 to 40 ns similar to under atmospheric conditions. The decay time is estimated to be around 40 ± 10 ns. Spin echoes show an exponential decay time of $3.3 \mu\text{s}$. Again, there is no significant influence of the trap on the spin properties, even under this low vacuum level, where other levitating schemes suffer from heating that impacts the NV photo-physical properties [23–26,53]. It is then likely that using purer samples, such as milled CVD diamonds [54–56] or dynamical decoupling techniques, will significantly increase the coherence time to milliseconds, very close to the oscillation frequency of our trapped diamonds.

Our results will find direct use in the field of spin optomechanics. A lot of effort is directed towards establishing a platform for coupling single spins to mechanical systems at the quantum level. Both tethered [8–10] and untethered [11–14] mechanical systems are being investigated. The latter makes use of single spins that are embedded in a moving particle in the presence of a fixed magnetic field. One promising way to establish strong coupling between the spin and mechanical d.o.f. is to couple NV centers to the rotational mode of a nanodiamond levitating in a Paul trap. The idea is to make use of the inherent quantization axis of the NV center to apply a torque to the whole nanodiamond. This can be done by coherently driving spin states dressed by a transverse magnetic field B in the angular sideband resolved regime [14]. The coupling rate is proportional to the single phonon

shift $\lambda_\phi = \gamma B \phi_0$, where γ is the gyromagnetic ratio of the electron and $\phi_0 = \sqrt{\hbar/2I\omega_\phi}$ is the ground state extension of the angular mode. I is the momentum of inertia, and ω_ϕ is the angular frequency of the considered rotational mode. The strong coupling condition is attained when the spin-coupling rate to the rotational mode is larger than the decoherence time of both the spin and the rotational mode.

To achieve this goal, the coherence time of the NV center should not be impacted by the trap and the mean particle angle should be locked to a given position. Our observation of long spin echoes under vacuum together with angular stability thus confirms that combining a Paul trap with spins in diamond is a viable option for such a spin-optomechanical scheme.

To contemplate coupling the motion of the particle to the spin now, the confinement frequency (at present in the kilohertz range) should be increased. It can be dramatically improved by reducing the trap size, raising back the voltage under high enough vacuum (see Sec. II of the SM [32]), and adding end-cap electrodes. One can then also reduce the size of the particle to increase the charge-to-mass ratio. Considering an prolate (aspect ratio 1:3) 180 nm diamond particle with a similar surface charge density to what we use here, in a $60 \mu\text{m}$ ring trap diameter and a peak voltage of up to 3000 V, the frequency of the highest rotational mode ω_ϕ is then expected to be around 100 kHz [14], which requires a T_2^* time of $10 \mu\text{s}$ to be in the sideband resolved regime. Using lower vacuum pressures to minimize collisions with gas particles and many NV centers [12] will then allow it to be well within the strong coupling regime.

We demonstrate efficient coherent control of the spin of NV centers inside a levitating diamond. Spin echoes are employed to show that the surface charges and the high electric potential difference between the diamond and the ring Paul trap do not impact the coherence time of the spins on microsecond timescales. Furthermore, the NV centers are used as motional probes for the levitating diamond. We could indeed identify a regime where the trap strongly stabilizes the particle angle under vacuum against the angular micromotion [14] and the laser radiation induced torque [31]. These results establish the Paul trap as a robust platform for precision manipulation and detection of trapped macroscopic objects using embedded atomlike emitters. Our demonstration of angular stability already opens a clear path towards strong coupling to the rotational d.o.f. [12,14]. A tantalizing prospect will be to use dynamical decoupling techniques [57] to bring the NV center's coherence time close to the millisecond-long T_1 time in order precisely measure the center-of-mass motion using magnetic field gradients. This will offer prospects to experiments such as matter wave interferometry [16,17], quantum gravity sensing [18], strong coupling [8,9], and cat state preparation [15] which rely on the ability to maintain long coherence times for spin-state superpositions in a trapped object.

We would like to acknowledge our fruitful discussions with Loic Rondin and Christophe Voisin. This research has been partially funded by the French National Research Agency (ANR) through the projects SMEQUI and QUOVADIS (T-ERC).

-
- [1] M. Aspelmeyer, T. J. Kippenberg, and F. Marquardt, *Rev. Mod. Phys.* **86**, 1391 (2014).
- [2] A. D. O'Connell, M. Hofheinz, M. Ansmann, R. C. Bialczak, M. Lenander, E. Lucero, M. Neeley, D. Sank, H. Wang, M. Weides *et al.*, *Nature (London)* **464**, 697 (2010).
- [3] J. D. Teufel, T. Donner, D. Li, J. W. Harlow, M. S. Allman, K. Cicak, A. J. Sirois, J. D. Whittaker, K. W. Lehnert, and R. W. Simmonds, *Nature (London)* **475**, 359 (2011).
- [4] S. Hong, R. Riedinger, I. Marinković, A. Wallucks, S. G. Hofer, R. A. Norte, M. Aspelmeyer, and S. Gröblacher, *Science* **358**, 203 (2017).
- [5] D. E. Chang, C. A. Regal, S. B. Papp, D. J. Wilson, J. Ye, O. Painter, H. J. Kimble, and P. Zoller, *Proc. Natl. Acad. Sci. U.S.A.* **107**, 1005 (2010).
- [6] O. Romero-Isart, A. C. Pflanzer, M. L. Juan, R. Quidant, N. Kiesel, M. Aspelmeyer, and J. I. Cirac, *Phys. Rev. A* **83**, 013803 (2011).
- [7] P. Treutlein, D. Hunger, S. Camerer, T. W. Hänsch, and J. Reichel, *Phys. Rev. Lett.* **99**, 140403 (2007).
- [8] P. Rabl, P. Cappellaro, M. V. G. Dutt, L. Jiang, J. R. Maze, and M. D. Lukin, *Phys. Rev. B* **79**, 041302 (2009).
- [9] O. Arcizet, V. Jacques, A. Siria, P. Poncharal, P. Vincent, and S. Seidelin, *Nat. Phys.* **7**, 879 (2011).
- [10] S. Kolkowitz, A. C. Bleszynski Jayich, Q. P. Unterreithmeier, S. D. Bennett, P. Rabl, J. G. E. Harris, and M. D. Lukin, *Science* **335**, 1603 (2012).
- [11] Y. Ma, T. M. Hoang, M. Gong, T. Li, and Z.-q. Yin, *Phys. Rev. A* **96**, 023827 (2017).
- [12] Z. Yin, N. Zhao, and T. Li, *Sci. China: Phys., Mech. Astron.* **58**, 1 (2015).
- [13] P. Kumar and M. Bhattacharya, *Opt. Express* **25**, 19568 (2017).
- [14] T. Delord, L. Nicolas, Y. Chassagneux, and G. Hétet, *Phys. Rev. A* **96**, 063810 (2017).
- [15] Z.-q. Yin, T. Li, X. Zhang, and L. M. Duan, *Phys. Rev. A* **88**, 033614 (2013).
- [16] M. Scala, M. S. Kim, G. W. Morley, P. F. Barker, and S. Bose, *Phys. Rev. Lett.* **111**, 180403 (2013).
- [17] C. Wan, M. Scala, G. W. Morley, A. T. M. A. Rahman, H. Ulbricht, J. Bateman, P. F. Barker, S. Bose, and M. S. Kim, *Phys. Rev. Lett.* **117**, 143003 (2016).
- [18] S. Bose, A. Mazumdar, G. W. Morley, H. Ulbricht, M. Toroš, M. Paternostro, A. A. Geraci, P. F. Barker, M. S. Kim, and G. Milburn, *Phys. Rev. Lett.* **119**, 240401 (2017).
- [19] O. Romero-Isart, M. L. Juan, R. Quidant, and J. I. Cirac, *New J. Phys.* **12**, 033015 (2010).
- [20] R. Kaltenbaek, G. Hechenblaikner, N. Kiesel, O. Romero-Isart, K. C. Schwab, U. Johann, and M. Aspelmeyer, *Exp. Astron.* **34**, 123 (2012).
- [21] M. Geiselmann, M. L. Juan, J. Renger, J. M. Say, L. J. Brown, F. J. G. de Abajo, F. Koppens, and R. Quidant, *Nat. Nanotechnol.* **8**, 175 (2013).
- [22] V. R. Horowitz, B. J. Alemn, D. J. Christle, A. N. Cleland, and D. D. Awschalom, *Proc. Natl. Acad. Sci. U.S.A.* **109**, 13493 (2012).
- [23] T. M. Hoang, J. Ahn, J. Bang, and T. Li, *Nat. Commun.* **7**, 12250 (2016).
- [24] L. P. Neukirch, E. von Haartman, J. M. Rosenholm, and N. Vamivakas, *Nat. Photonics* **9**, 653 (2015).
- [25] T. Delord, L. Nicolas, M. Bodini, and G. Hétet, *Appl. Phys. Lett.* **111**, 013101 (2017).
- [26] R. M. Pettit, L. P. Neukirch, Y. Zhang, and A. N. Vamivakas, *J. Opt. Soc. Am. B* **34**, C31 (2017).
- [27] S. D. Bennett, S. Kolkowitz, Q. P. Unterreithmeier, P. Rabl, A. C. B. Jayich, J. G. E. Harris, and M. D. Lukin, *New J. Phys.* **14**, 125004 (2012).
- [28] H. Straubel, *Naturwissenschaften* **42**, 506 (1955).
- [29] N. Yu, W. Nagourney, and H. Dehmelt, *J. Appl. Phys.* **69**, 3779 (1991).
- [30] W. Paul, *Rev. Mod. Phys.* **62**, 531 (1990).
- [31] T. Delord, L. Nicolas, L. Schwab, and G. Hétet, *New J. Phys.* **19**, 033031 (2017).
- [32] See Supplemental Material at <http://link.aps.org/supplemental/10.1103/PhysRevLett.121.053602>, which includes Refs. [33–40], for a discussion on the width and contrast of the ESR and on the influence of the green laser on the ESR and diamond motion.
- [33] J.-P. Tetienne, L. Rondin, P. Spinicelli, M. Chipaux, T. Debuisschert, J.-F. Roch, and V. Jacques, *New J. Phys.* **14**, 103033 (2012).
- [34] J. R. Maze, A. Dréau, V. Waselowski, H. Duarte, J.-F. Roch, and V. Jacques, *New J. Phys.* **14**, 103041 (2012).
- [35] N. Zhao, S.-W. Ho, and R.-B. Liu, *Phys. Rev. B* **85**, 115303 (2012).
- [36] V. Jain, J. Gieseler, C. Moritz, C. Dellago, R. Quidant, and L. Novotny, *Phys. Rev. Lett.* **116**, 243601 (2016).
- [37] L. Jiang, M. V. G. Dutt, E. Togan, L. Childress, P. Cappellaro, J. M. Taylor, and M. D. Lukin, *Phys. Rev. Lett.* **100**, 073001 (2008).
- [38] Y. Roichman, B. Sun, A. Stolarski, and D. G. Grier, *Phys. Rev. Lett.* **101**, 128301 (2008).
- [39] P. Wu, R. Huang, C. Tischer, A. Jonas, and E.-L. Florin, *Phys. Rev. Lett.* **103**, 108101 (2009).
- [40] T. Li, *Fundamental Tests of Physics with Optically Trapped Microspheres* (Springer, New York, 2013), p. 81.
- [41] A. Kuhlicke, A. W. Schell, J. Zoll, and O. Benson, *Appl. Phys. Lett.* **105**, 073101 (2014).
- [42] A. Dréau, M. Lesik, L. Rondin, P. Spinicelli, O. Arcizet, J.-F. Roch, and V. Jacques, *Phys. Rev. B* **84**, 195204 (2011).
- [43] K. Jensen, V. M. Acosta, A. Jarmola, and D. Budker, *Phys. Rev. B* **87**, 014115 (2013).
- [44] A. Jarmola, V. M. Acosta, K. Jensen, S. Chemerisov, and D. Budker, *Phys. Rev. Lett.* **108**, 197601 (2012).
- [45] N. Bar-Gill, L. M. Pham, A. Jarmola, D. Budker, and R. L. Walsworth, *Nat. Commun.* **4**, 1743 (2013).
- [46] J.-P. Tetienne, T. Hingant, L. Rondin, A. Cavaillès, L. Mayer, G. Dantelle, T. Gacoin, J. Wrachtrup, J.-F. Roch, and V. Jacques, *Phys. Rev. B* **87**, 235436 (2013).
- [47] L. Viola and S. Lloyd, *Phys. Rev. A* **58**, 2733 (1998).
- [48] V. V. Dobrovitski, A. E. Feiguin, R. Hanson, and D. D. Awschalom, *Phys. Rev. Lett.* **102**, 237601 (2009).

- [49] V. V. Dobrovitski, A. E. Feiguin, D. D. Awschalom, and R. Hanson, *Phys. Rev. B* **77**, 245212 (2008).
- [50] E. I. Baibekov, *JETP Lett.* **93**, 292 (2011).
- [51] R. Boscaino, F. M. Gelardi, and J. P. Korb, *Phys. Rev. B* **48**, 7077 (1993).
- [52] P. L. Stanwix, L. M. Pham, J. R. Maze, D. Le Sage, T. K. Yeung, P. Cappellaro, P. R. Hemmer, A. Yacoby, M. D. Lukin, and R. L. Walsworth, *Phys. Rev. B* **82**, 201201 (2010).
- [53] D. M. Toyli, D. J. Christle, A. Alkauskas, B. B. Buckley, C. G. Van de Walle, and D. D. Awschalom, *Phys. Rev. X* **2**, 031001 (2012).
- [54] J. Millen, T. Deesuwan, P. Barker, and J. Anders, *Nat. Nanotechnol.* **9**, 425 (2014).
- [55] A. T. M. A. Rahman, A. C. Frangeskou, M. S. Kim, S. Bose, G. W. Morley, and P. F. Barker, *Sci. Rep.* **6**, 21633 (2016).
- [56] A. C. Frangeskou, A. T. M. A. Rahman, L. Gines, S. Mandal, O. A. Williams, P. F. Barker, and G. W. Morley, *New J. Phys.* **20**, 043016 (2018).
- [57] G. de Lange, Z. H. Wang, D. Ristè, V. V. Dobrovitski, and R. Hanson, *Science* **330**, 60 (2010).